Supplemental Tables

Table S1: Fluorescent spore assay data.

Table S2: Yeast two-hybrid interactions between mammalian SC central element proteins and TEX11 (Xcel spreadsheet).

Table S3: Yeast strains used (Xcel spreadsheet).

Supplemental figures legends

Figure S1: Heatmap showing the enrichment of Ecm11 at DSB hotspots and Red1 axis-attachment sites

Same data as those shown in Fig. 1D. Each line represents one site of the indicated class. Average nomalized Ecm11 reads numbers is indicated by a color scale (on the right)

Figure S2: Zip4 binding to chromosomes is reduced in absence of Zip1 protein

ChIP monitoring of Zip4-Flag association with different chromosomal regions, measured by qPCR using primers that cover the indicated regions. Values are the mean ± SEM of at least three independent experiments. The graph on the right represents a magnification of the central graph.

Figure S3: Zip4 interacts with Ecm11 through an aromatic-asparagine motif

A. Yeast two-hybrid interaction analysis between truncated Zip4 and Ecm11. Preys and baits are fused with the GAL4 Activation Domain (GAL4-AD) and with the GAL4 DNA-Binding Domain (GAL4-BD), respectively. The green frame indicates the interaction between Zip4-875-975 and Ecm11.

B. Yeast two-hybrid interaction analysis between Zip4 and Ecm11/Zip2. The blue frame indicates the absence of interaction between Zip4N919Q and Ecm11.

A-B: The interaction is revealed by growth on the selective –His/Ade medium.

Figure S4: Delineation of the Ecm11 region interacting with Zip4

A. Illustration of the predicted structure of Zip4 WN motif interacting with Ecm11.

B. Multiple sequence alignment gathering homologs of Ecm11 in budding yeasts of the *Saccharomycetaceae* family (22 sequences with their NCBI identifiers and delimitation index indicated). The conserved SUMOylation site containing the modified Lysine 5 is highlighted in the cyan box. The N-terminal region interacting with Zip4 and predicted to adopt a small helical conformation is boxed in magenta with the conserved positions of L69 and L73 highlighted. The C-terminal region predicted to form a coiled-coil over 63 residues is indicated by the orange box. Blue vertical lines indicate the positions of long insertions present in only a few homologs of *S. cerevisiae* Ecm11 which were masked for the sake of compact representation.

C. Yeast two-hybrid self-interaction analysis of Ecm11. Same legend as in Fig. S3.

Figure S5: *zip4N919Q* and *ecm11LLDD* phenotype in meiosis

A. Meiotic progression assessed by DAPI-staining of the strains with the indicated genotype. Values are the mean ± SEM of at least three independent experiments (except for ecm11LLDD-Myc: ±SD from two independent experiments).

B. Western blot time course analysis of Zip4-Flag or Zip4N919Q-Flag (upper panel) or Zip4-Flag in *ECM11* or *ecm11Δ* strain (lower panel), and. Right: quantifications of Zip4-Flag signal, relative to Pgk1.

C. ChIP monitoring of Ecm11-Flag in the indicated strains and Ecm11LLDD-Flag association with different chromosomal regions, measured by qPCR using primers that

cover the indicated regions. Values are the mean ± SEM of at least three independent experiments.

Figure S6: Localization of Ecm11-Myc on meiotic spreads.

Ecm11-Myc localization on surface-spread chromosomes in the indicated strains. Red: anti-Myc; green: anti-Red1; blue: DAPI. The description of the categories is in Fig. 3C

Figure S7: Zip1 staining and meiotic recombination after tethering Ecm11LLDD to Zip4.

A. Zip1 localization on surface-spread chromosomes in the indicated conditions (- and + rapamycin) at 4, 5 and 6 hours after meiosis induction. Only pachytene or pachytene-like stages are considered. Green: anti-Zip1; blue: DAPI.

B. Quantification of Zip1 signal intensity observed in A. ****: p-value<0.0001, Wilcoxon test.

C. Quantification of DAPI-positive spreads showing a polycomplex. At least 200 spreads were considered for each condition. Values are % cells ± SD of the proportion.

D. Spore viability in the indicated conditions (- and + rapamycin) 72 h after meiosis induction

E-F. Crossing-over frequency and MI non disjunction. Same experimental setup as in Fig. 4. Genetic distances in the two genetic intervals *CEN8-ARG4* and *ARG4-THR1* on chromosome VIII are plotted as cM ± SE for the indicated genotypes. ****: p-value<0.0001, G-test. WT and ecm11Δ are the same data as in Fig. 3.

G: Pulsed-field gel analysis of DSB formation with a probe located at the left end of chromosome 8. The bracket indicates the DSB region that was quantified over the total signal in each lane.

Figure S8: Modelling the assembly of the Gmc2-Ecm11 complex using constraints of deep learning-enhanced covariation-based prediction methods reveals similarities with the assembly of the TEX12-SYCE2 hetero-tetrameric coiled-coils.

A. A co-multiple sequence alignment (co-MSA) containing 451 non-redundant pairs of fungal sequences homologous to *S. cerevisiae* Gmc2 and Ecm11 was concatenated and used as input of RaptorX contact prediction method (see Materials and Methods). B. The same protocol was performed with homologs of human SYCE2 and TEX12 using a 135-sequences co-MSA.

C. The contact maps predicted by RaptorX for Gmc2-Ecm11 are shown with a grey-scale representing contacts probabilities. Coloured boxes indicate the predicted intra-molecular contacts while the contacts outside the coloured boxes report the inter-molecular predicted contacts. Inter-molecular contacts are predicted significantly stronger with co-existence of anti-parallel (orange) and parallel (light orange) coiled-coils. RaptorX constraints with succession of anti-parallel and parallel coiled-coils could only be respected assuming a dimer of heterodimer for Gmc2-Ecm11 subunits, to build the 3D model (See Fig. 6D).

D. The same predictions were also run to predict the contact map for the SYCE2-TEX12 complex.

E. Analysis of the consistency between the contacts maps predicted using RaptorX and the 3D model of the Gmc2-Ecm11 complex shown in Fig. 6D (black curve) or the structure of the SYCE2-TEX12 complex shown in Fig. 6C (grey curve). The curves report the ratio of satisfied contacts between residues (distance Cb-Cb < 8Å) among the top N predicted contacts sorted by decreasing probabilities. The plots span the best 200 contacts. For

both the crystal structure of SYCE2-TEX12 complex and the model of Gmc2-Ecm11, we observe that about 90% of the top50 predicted contacts are correct or can be satisfied, respectively. This comparison establishes the likelihood of the proposed assembly mode for the Gmc2-Ecm11 complex.

Table S1

Genotype	Reference interval	Test interval	CEN8-ARG4 ARG4-THR1	ARG4-THR1 CEN8-ARG4
Wild-type	TT+NPD	PD:NPD:TT	1048:0:62	508:0:62
		cM ± SE	2.79 ± 0.34	5.44 ± 0.65
	PD	PD:NPD:TT	2149:0:508	2149:10:1038
		cM ± SE	9.56 ± 0.38	17.17 ± 0.50
	ratio		0.29	0.32
	p-value		0	0
	total	PD:NPD:TT	3197:0:570	2657:10:1100
		cM ± SE	7.57 ± 0.29	15.40 ± 0.44
	p-value	vs WT	-	-
		vs *ecm11*Δ	0.151	0.0687
		vs *zip4N919Q*	0.151	0
		vs *zip4*Δ	7.14E-09	0
***ecm11*Δ**	TT+NPD	PD:NPD:TT	692:0:77	397:0:77
		cM ± SE	5.01 ± 0.54	8.12 ± 0.85
	PD	PD:NPD:TT	1631:0:397	1631:13:679
		cM ± SE	9.79 ± 0.44	16.29 ± 0.65
	ratio		0.51	0.50
	p-value		2.62E-09	6.56E-10
	total	PD:NPD:TT	2323:0:474	2028:13:756
		cM ± SE	8.47 ± 0.35	14.91 ± 0.56
	p-value	vs WT	0.151	0.0687
		vs *ecm11*Δ	-	-
		vs *zip4N919Q*	0.00174	0
		vs *zip4*Δ	3.31E-11	0
zip4N919Q	TT+NPD	PD:NPD:TT	391:0:42	343:0:42
		cM ± SE	4.85 ± 0.71	5.45 ± 0.79
	PD	PD:NPD:TT	2088:0:343	2088:5:386
		cM ± SE	7.05 ± 0.35	8.39 ± 0.45
	ratio		0.69	0.65
	p-value		0.0367	0.022
	total	PD:NPD:TT	2479:0:385	2431:5:428
		cM ± SE	6.72 ± 0.32	8.00 ± 0.40
	p-value	vs WT	0.151	0
		vs *ecm11*Δ	0.00174	0
		vs *zip4N919Q*	-	-
		vs *zip4*Δ	2.92E-06	5.48E-09

***zip4*Δ**	TT+NPD	PD:NPD:TT	39:0:5	34:0:5
		cM ± SE	5.68 ± 2.39	6.41 ± 2.68
	PD	PD:NPD:TT	533:0:34	533:4:35
		cM ± SE	3.00 ± 0.50	5.16 ± 1.15
	ratio		1.90	1.24
	p-value		0.439	0.264
	total	PD:NPD:TT	572:0:39	567:4:40
		cM ± SE	3.19 ± 0.49	5.24 ± 1.09
	p-value	vs WT	7.14E-09	0
		vs *ecm11*Δ	3.31E-11	0
		vs *zip4N919Q*	2.92E-06	5.48E-09
		vs *zip4*Δ	-	-

ZIP4-FKPB12
ecm11LLDD-FRB

-rapamycin	TT+NPD	PD:NPD:TT	893:0:154	554:0:154
		cM ± SE	7.35 ± 0.55	10.88 ± 0.78
	PD	PD:NPD:TT	2079:0:554	2079:9:884
		cM ± SE	10.52 ± 0.40	15.78 ± 0.51
	ratio		0.70	0.69
	p-value		4.20E-05	9.97E-06
	total	PD:NPD:TT	2972:0:708	2633:9:1038
		cM ± SE	9.62 ± 0.32	14.84 ± 0.44
	p-value	vs WT	2.35E-05	0.624
		vs *ecm11*Δ	7.20E-02	0.238
		vs +rapamycin	0	0

+rapamycin	TT+NPD	PD:NPD:TT	354:0:28	229:0:28
		cM ± SE	3.66 ± 0.67	5.45 ± 0.97
	PD	PD:NPD:TT	2469:0:229	2469:31:323
		cM ± SE	4.24 ± 0.27	9.02 ± 0.65
	ratio		0.86	0.60
	p-value		0.738	0.0628
	total	PD:NPD:TT	2823:0:257	2698:31:351
		cM ± SE	4.17 ± 0.25	8.72 ± 0.60
	p-value	vs WT	0	0
		vs *ecm11*Δ	0	0
		vs -rapamycin	0	0

Genetic distances were compared by applying the G test to the distribution of parental ditype (PD), non-parental ditype (NPD) and tetratype (TT).

Genotype		MI nondisjunction	
Wild-type		MI nondisj:MI disj	12:3767
		% MI nondisj	0.32
		95 % CI (%)	(0.55, 0.18)
	p-value	vs WT	-
		vs *ecm11*Δ	0.00122
		vs *zip4*Δ	6.96E-76
***ecm11*Δ**		MI nondisj:MI disj	27:2797
		% MI nondisj	0.96
		95 % CI (%)	(1.39, 0.66)
	p-value	vs WT	0.00122
		vs *ecm11*Δ	-
		vs *zip4*Δ	3.87E-53
zip4N919Q		MI nondisj:MI disj	42:2864
		% MI nondisj	1.45
		95 % CI (%)	(1.95, 1.07)
	p-value	vs WT	7.89E-07
		vs *ecm11*Δ	0.115
		vs *zip4*Δ	2.64E-46
***zip4*Δ**		MI nondisj:MI disj	120:611
		% MI nondisj	16.42
		95 % CI (%)	(19.3, 13.91)
	p-value	vs WT	6.96E-76
		vs *ecm11*Δ	3.87E-53
		vs *zip4*Δ	-

ZIP4-FKPB12
ecm11LLDD-FRB

- rapamycin

	MI nondisj:MI disj	19:3680
	% MI nondisj	0.51
	95 % CI (%)	(0.80, 0.33)
p-value	vs WT	2.11E-01
	vs *ecm11*Δ	4.50E-02
	vs +rapamycin	7.67E-67

+ rapamycin

	MI nondisj:MI disj	290:3080
	% MI nondisj	8.61
	95 % CI (%)	(9.60, 7.70)
p-value	vs WT	2.03E-74
	vs *ecm11*Δ	3.82E-45
	vs -rapamycin	7.67E-67

%MI nondisjunction were compared by applying the Fisher test to the number of MI nondisjunctions and MI disjunctions.

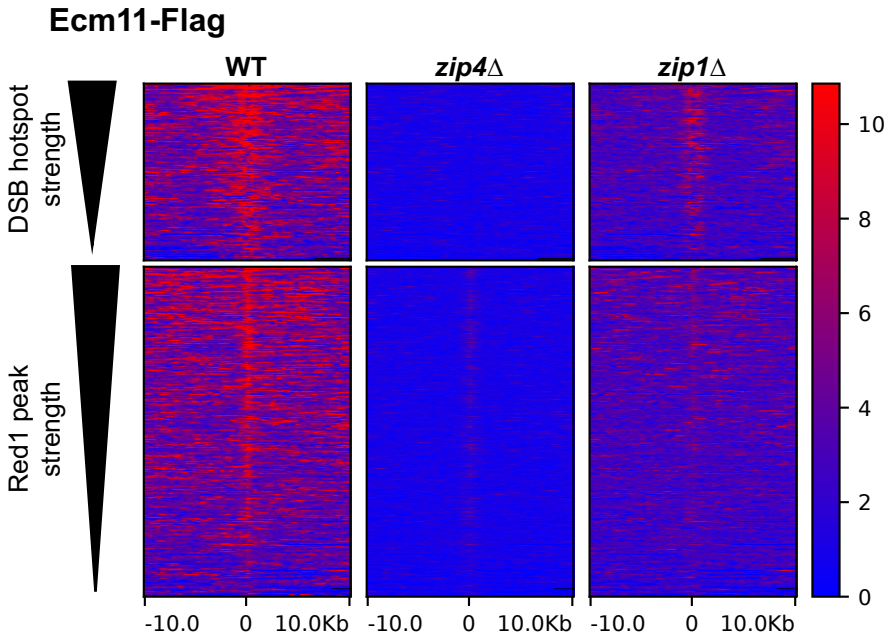
Ecm11-Flag
WT
zip4Δ
zip1Δ
DSB hotspot strength
Red1 peak strength
10
8
6
4
2
0
-10.0
0
10.0Kb
-10.0
0
10.0Kb
-10.0
0
10.0Kb

Fig.S1

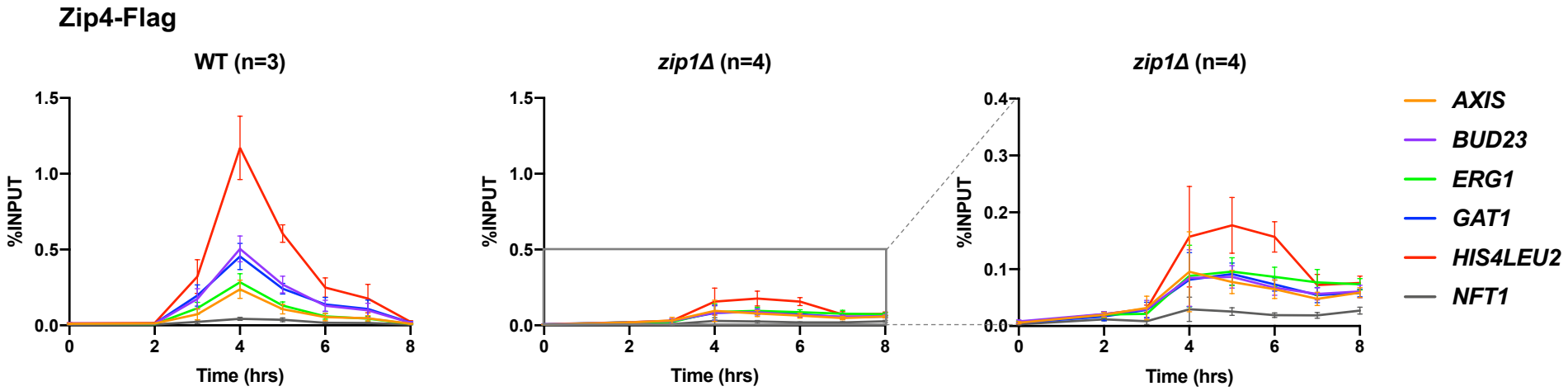
Zip4-Flag
WT (n=3)
zip1Δ (n=4)
zip1Δ (n=4)
%INPUT
Time (hrs)
AXIS
BUD23
ERG1
GAT1
HIS4LEU2
NFT1

Fig.S2

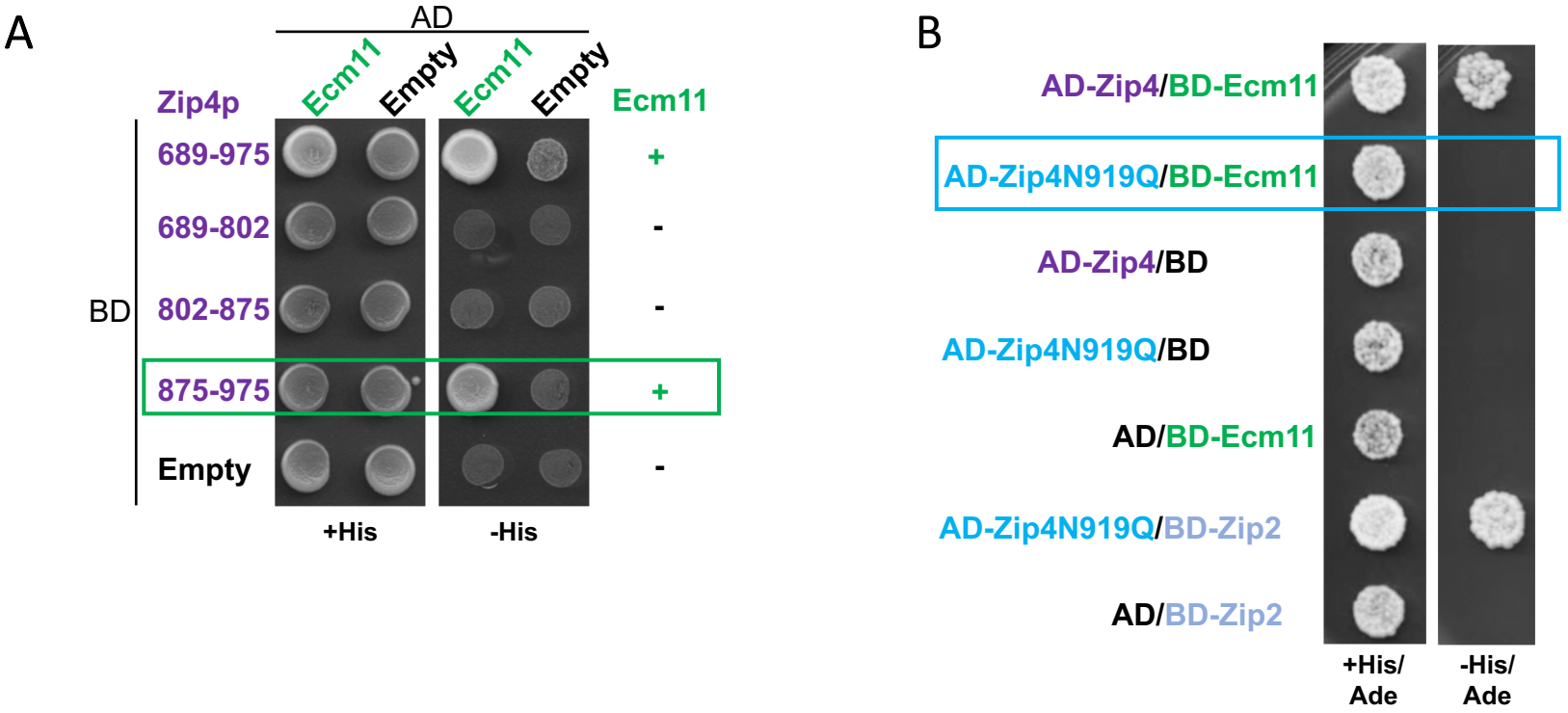
A
AD
Ecm11
Empty
Ecm11
Empty
Zip4p
Ecm11
BD
689-975
689-802
802-875
875-975
Empty
+
-
-
+
-
+His
-His
B
AD-Zip4/BD-Ecm11
AD-Zip4N919Q/BD-Ecm11
AD-Zip4/BD
AD-Zip4N919Q/BD
AD/BD-Ecm11
AD-Zip4N919Q/BD-Zip2
AD/BD-Zip2
+His/
Ade
-His/
Ade

Fig.S3

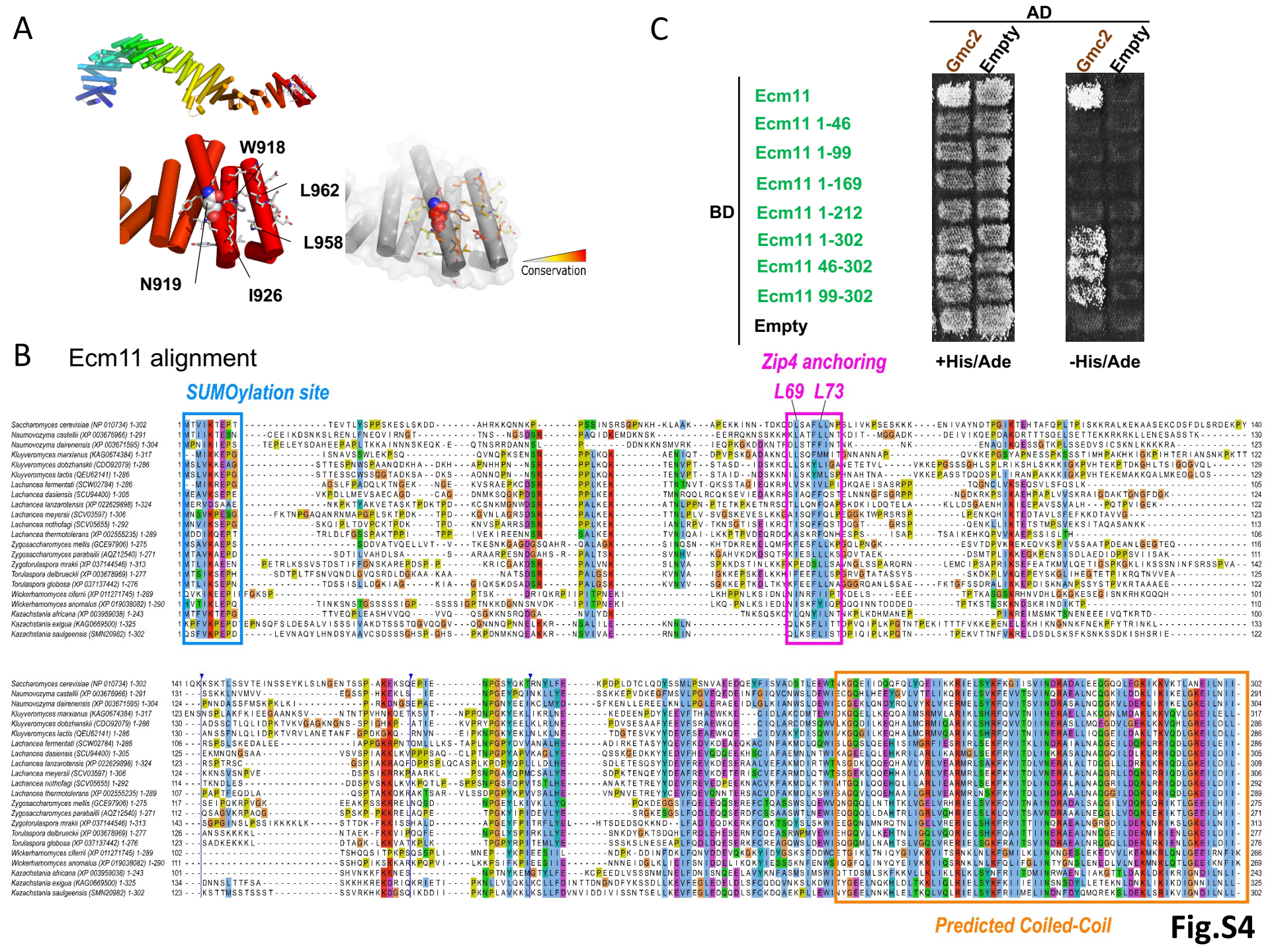
A
W918
L962
L958
N919
I926
Conservation
C
AD
Gmc2
Empty
Gmc2
Empty
BD
Ecm11
Ecm11 1-46
Ecm11 1-99
Ecm11 1-169
Ecm11 1-212
Ecm11 1-302
Ecm11 46-302
Ecm11 99-302
Empty
+His/Ade
-His/Ade
B
Ecm11 alignment
SUMOylation site
Zip4 anchoring
L69 L73
Saccharomyces cerevisiae (NP 010734) 1-302
Naumovozyma castellii (XP 003676966) 1-291
Naumovozyma dairenensis (XP 003671595) 1-304
Kluyveromyces marxianus (KAG0674384) 1-317
Kluyveromyces dobzhanskii (CDQ09279) 1-286
Kluyveromyces lactis (QEU62141) 1-286
Lachancea fermentati (SCW02784) 1-286
Lachancea dasiensis (SCU94400) 1-305
Lachancea lanzarotensis (XP 022629898) 1-324
Lachancea meyersii (SCV03597) 1-306
Lachancea nothofagi (SCV05655) 1-292
Lachancea thermotolerans (XP 002555235) 1-289
Zygosaccharomyces mellis (GCE97906) 1-275
Zygosaccharomyces parabailii (AQZ12540) 1-271
Zygotorulaspora mrakii (XP 037144546) 1-313
Torulaspora delbrueckii (XP 003678969) 1-277
Torulaspora globosa (XP 037137442) 1-276
Wickerhamomyces ciferrii (XP 011271745) 1-289
Wickerhamomyces anomalus (XP 019038082) 1-290
Kazachstania africana (XP 003959038) 1-243
Kazachstania exigua (KAG0669500) 1-325
Kazachstania saulgeensis (SMN20982) 1-302
Predicted Coiled-Coil
Fig.S4

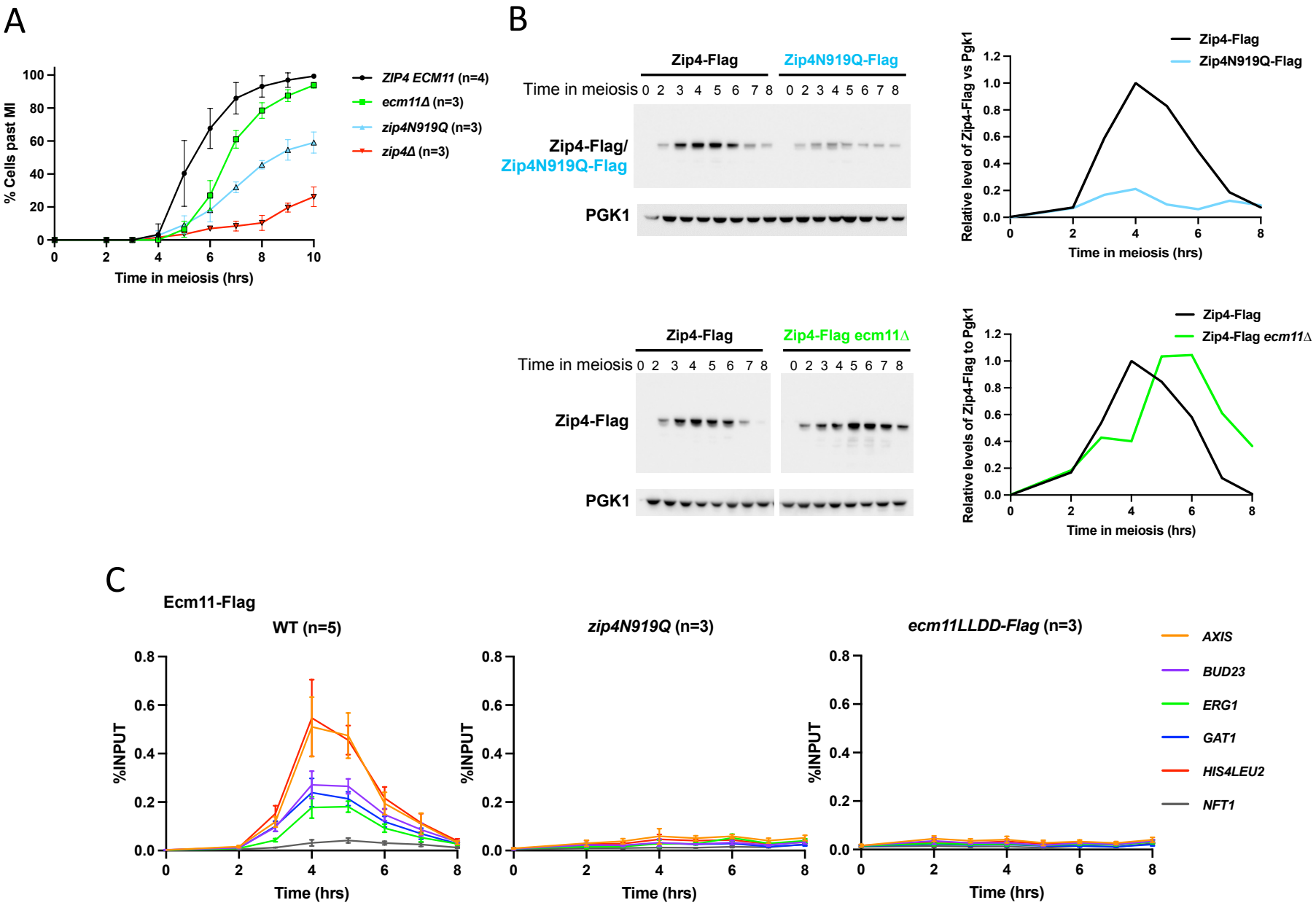
A
% Cells past MI
Time in meiosis (hrs)
ZIP4 ECM11 (n=4)
ecm11Δ (n=3)
zip4N919Q (n=3)
zip4Δ (n=3)
B
Zip4-Flag
Zip4N919Q-Flag
Time in meiosis 0 2 3 4 5 6 7 8 0 2 3 4 5 6 7 8
Zip4-Flag/ Zip4N919Q-Flag
PGK1
Relative level of Zip4-Flag vs Pgk1
Time in meiosis (hrs)
Zip4-Flag
Zip4-Flag ecm11Δ
Time in meiosis 0 2 3 4 5 6 7 8 0 2 3 4 5 6 7 8
Zip4-Flag
PGK1
Relative levels of Zip4-Flag to Pgk1
Time in meiosis (hrs)
C
Ecm11-Flag
WT (n=5)
zip4N919Q (n=3)
ecm11LLDD-Flag (n=3)
%INPUT
Time (hrs)
AXIS
BUD23
ERG1
GAT1
HIS4LEU2
NFT1

Fig.S5

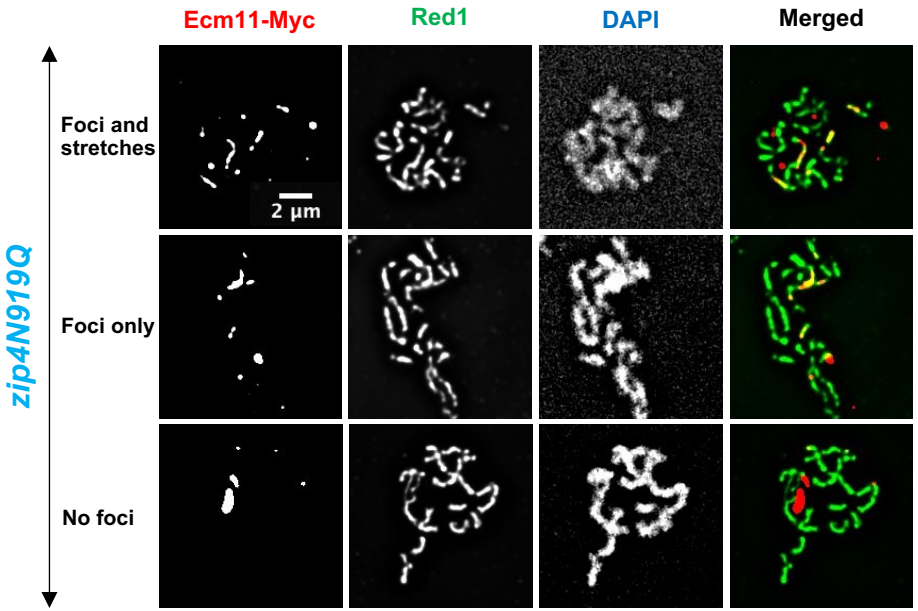
Ecm11-Myc
Red1
DAPI
Merged
zip4N919Q
Foci and stretches
Foci only
No foci
2 µm

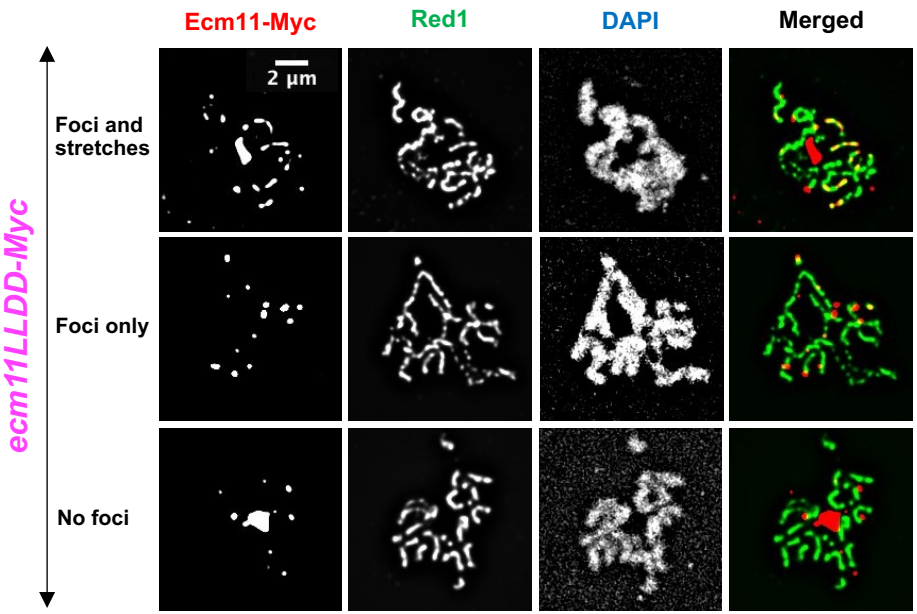
Ecm11-Myc
Red1
DAPI
Merged
ecm11LLDD-Myc
Foci and stretches
Foci only
No foci
2 µm

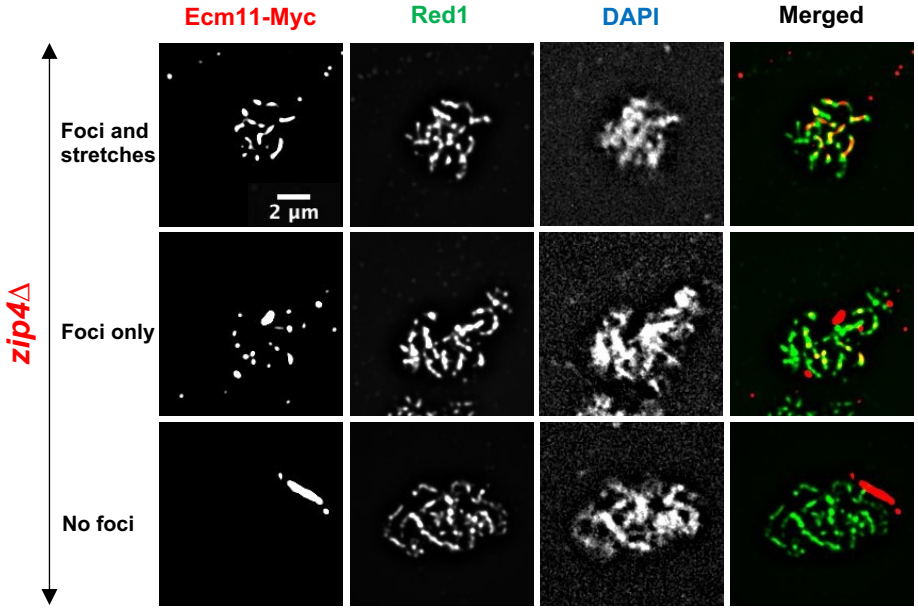
Ecm11-Myc
Red1
DAPI
Merged
zip4Δ
Foci and stretches
Foci only
No foci
2 µm

Fig.S6

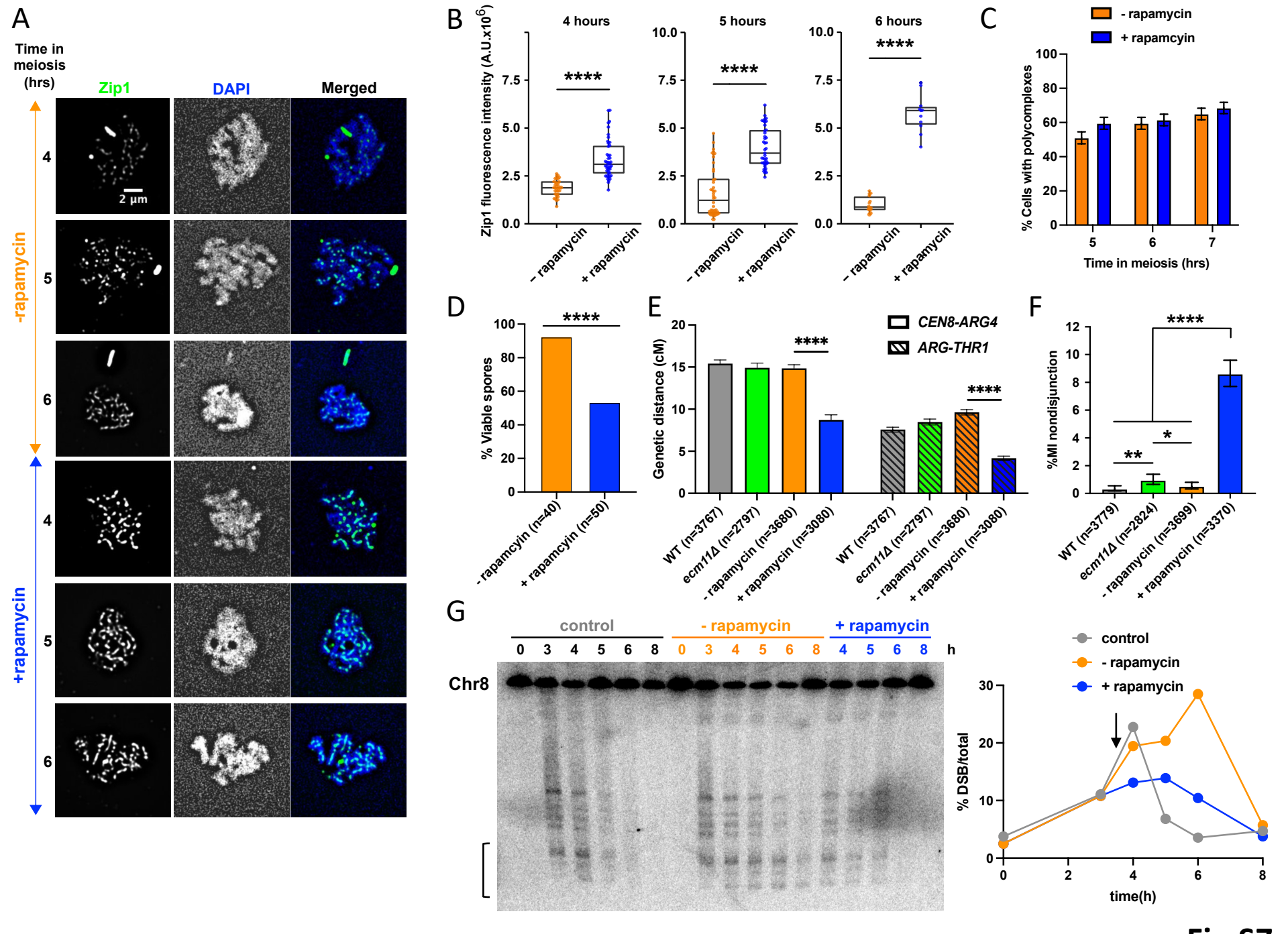
A
Time in meiosis (hrs)
Zip1
DAPI
Merged
-rapamycin
+rapamycin
4
5
6
4
5
6
2 µm
B
4 hours
5 hours
6 hours
Zip1 fluorescence intensity (A.U.x10^6)
****
- rapamycin
+ rapamycin
C
- rapamycin
+ rapamcyin
% Cells with polycomplexes
Time in meiosis (hrs)
D
% Viable spores
- rapamcyin (n=40)
+ rapamcyin (n=50)
E
CEN8-ARG4
ARG-THR1
Genetic distance (cM)
WT (n=3767)
ecm11Δ (n=2797)
- rapamycin (n=3680)
+ rapamycin (n=3080)
F
%MI nondisjunction
**
*
WT (n=3779)
ecm11Δ (n=2824)
- rapamycin (n=3699)
+ rapamycin (n=3370)
G
control
- rapamycin
+ rapamycin
0 3 4 5 6 8 0 3 4 5 6 8 4 5 6 8 h
Chr8
% DSB/total
time(h)

Fig.S7

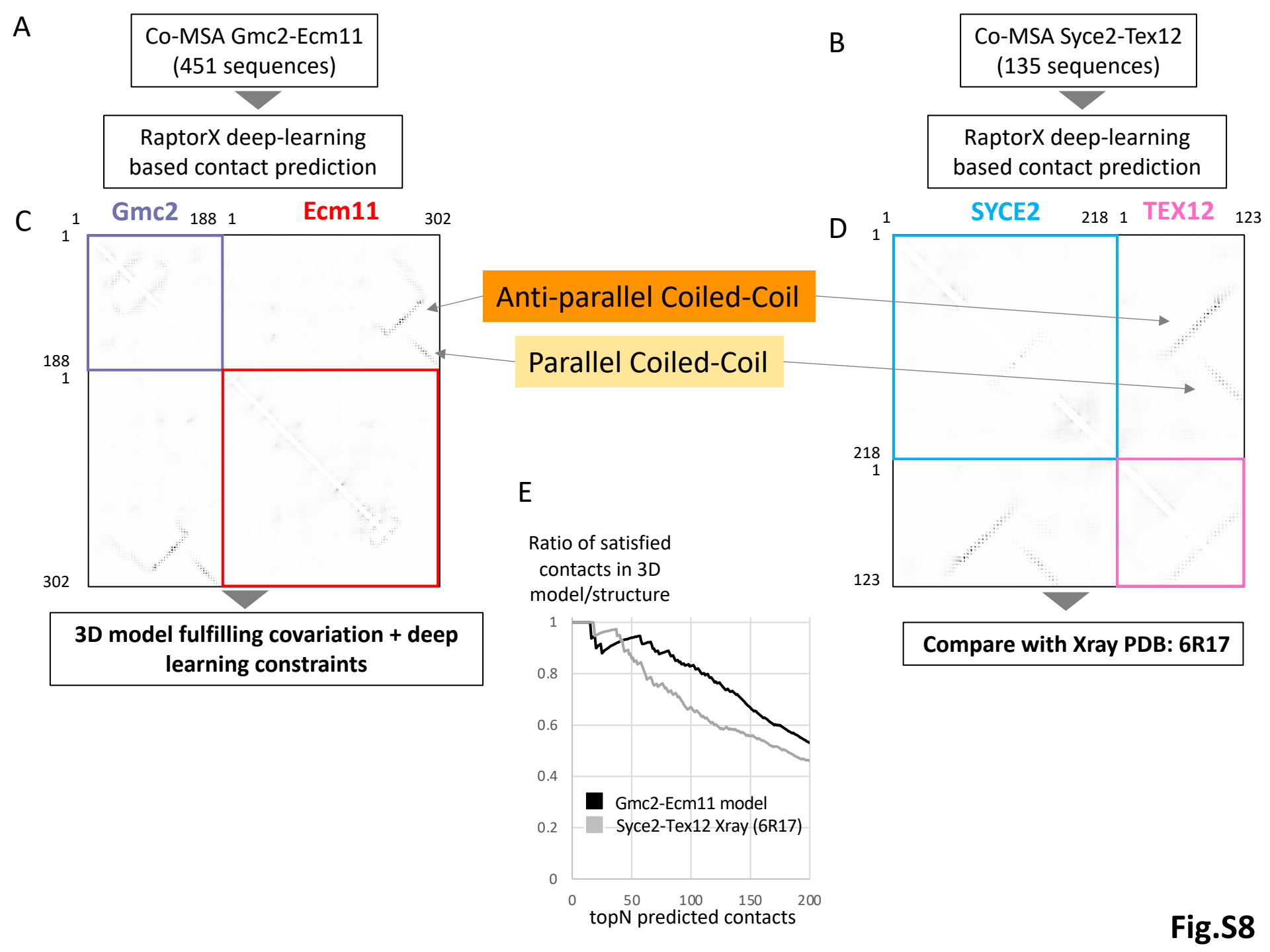
A
Co-MSA Gmc2-Ecm11
(451 sequences)
RaptorX deep-learning
based contact prediction
B
Co-MSA Syce2-Tex12
(135 sequences)
RaptorX deep-learning
based contact prediction
C
Gmc2
Ecm11
1
188
1
302
D
SYCE2
TEX12
218
123
Anti-parallel Coiled-Coil
Parallel Coiled-Coil
3D model fulfilling covariation + deep learning constraints
Compare with Xray PDB: 6R17
E
Ratio of satisfied contacts in 3D model/structure
Gmc2-Ecm11 model
Syce2-Tex12 Xray (6R17)
topN predicted contacts
Fig.S8